ANTIOXIDANTS & REDOX SIGNALING
Volume 13, Number 12, 2010
© Mary Ann Liebert, Inc.
DOI: 10.1089/ars.2010.3104

Factors Released from Embryonic Stem Cells Stimulate c-kit-FLK-1^{+ve} Progenitor Cells and Enhance Neovascularization

Sumbul Fatma,[1,*] Donald E. Selby,[2,*] Reetu D. Singla,[1] and Dinender K. Singla[1]

Abstract

We examined whether factors released from embryonic stem (ES) cells inhibit cardiac and vascular cell apoptosis and stimulate endogenous progenitor cells that enhance neovascularization with improved cardiac function. We generated and transplanted ES-conditioned medium (CM) in the infarcted heart to examine effects on cardiac and vascular apoptosis, activation of endogenous c-kit and FLK-1^{+ve} cells, and their role in cardiac neovascularization. TUNEL, caspase-3 activity, immunohistochemistry, H&E, and Masson's trichrome stains were used to determine the effect of transplanted ES-CM on cardiac apoptosis and neovascularization. TUNEL staining and caspase-3 activity confirm significantly ($p < 0.05$) reduced apoptosis in MI+ES-CM compared with MI+ cell culture medium. Immunohistochemistry demonstrated increased ($p < 0.05$, 53%) c-kit^{+ve} and FLK-1^{+ve} positive cells, as well as increased ($p < 0.05$, 67%) differentiated CD31-positive cells in ES-CM groups compared with respective controls. Furthermore, significantly ($p < 0.05$) increased coronary artery vessels were observed in ES-CM transplanted hearts compared with control. Heart function was significantly improved following ES-CM transplantation. Next, we observed significantly increased ($p < 0.05$) levels of c-kit activation proteins (HGF and IGF-1), anti-apoptosis factors (IGF-1 and total antioxidants), and neovascularization protein (VEGF). In conclusion, we suggest that ES-CM following transplantation in the infarcted heart inhibits apoptosis, activates cardiac endogenous c-kit and FLK-1^{+ve} cells, and differentiates them into endothelial cells (ECs) that enhances neovascularization with improved cardiac function. *Antioxid. Redox Signal*. 13, 1857–1865.

Introduction

MYOCARDIAL INFARCTION (MI) induces irreversible loss of myocytes and vascular cells within the infarct and peri-infarct regions, leading to cardiovascular remodeling and ultimately, end stage heart failure and death (2, 4, 17, 19). Novel cell transplantation approaches have been examined to regenerate and repair injured myocardium (3, 10, 11, 27, 28). Many different cell types such as bone marrow stem cells, neonatal cardiac myocytes, ventricular cardiomyocytes, skeletal myoblasts, smooth muscle cells, fetal cardiac myocytes, mesenchymal stem cells (MSCs), and mouse and human embryonic stem (ES) cells were transplanted in various animal models to regenerate injured myocardium (3, 10, 11, 27, 28). We and others demonstrated that mouse ES cells transplanted after MI in the heart can differentiate into cardiac myocytes (18, 23, 28). Furthermore, we also suggested that transplanted ES cells differentiate into vascular smooth muscle and endothelial cells (ECs), suggesting neovascularization may contribute to improved cardiac function (18, 23, 28). Both adult and ES cell transplantation studies indicate that improved cardiac function is associated with myogenesis and neovascularization (11, 18, 23, 28).

Autocrine or paracrine factors released from MSCs following transplantation in the infarcted heart inhibit cardiac myocyte apoptosis and improve function (7, 8). Furthermore, we developed oxidative stress-induced apoptosis in H9c2 cells and demonstrated that factors released from ES cells inhibit apoptosis in the cell culture model (30, 31). However, whether factors released from ES cells can inhibit apoptosis and enhance neovascularization following transplantation in the infarcted mouse heart remains unknown.

Accordingly, we hypothesized that transplanted factors released from ES cells in the infarcted heart inhibit apoptosis, enhance neovascularization, and improve cardiac function. To test this hypothesis, we generated conditioned medium (CM) from cultured ES cells and transplanted it in the infarcted mouse heart. We demonstrate that released factors in

[1]Burnett School of Biomedical Sciences, College of Medicine, University of Central Florida, Orlando, Florida.
[2]Department of Medicine, University of Vermont, Burlington, Vermont.
*These authors contributed equally to this work.

ES-CM following transplantation inhibit cardiac apoptosis, activate endogenous c-kit^{+ve}-fetal liver kinase (FLK1^{+ve}) progenitor cells, and enhance neovascularization post-MI.

Materials and Methods

Preparation of ES-CM

Mouse ES cells were maintained in Dulbecco's minimum essential medium (DMEM, Invitrogen, Carlsbad, CA) supplemented with sodium pyruvate, leukemia inhibitory factor (LIF), glutamine, penicillin-streptomycin, β-mercaptoethanol, nonessential amino acids, and 15% FBS (Invitrogen) as we previously reported (30, 31). ES-CM was prepared by growing 9000 ES cells/cm^2 in Petri dishes containing cell culture medium with LIF for 24 h and then replaced with fresh cell culture medium without LIF for 48 h (30, 31). After 48 h, cell culture supernatants (CM) from growing ES cells were collected and labeled as ES-CM as reported previously (30, 31). To prepare 15× concentrated ES-CM we used Centriprep filter devices (Billerica, MA). In brief, 15 ml of ES-CM was poured onto Centriprep filter and the cap was closed provided with the tubes. Centrifugation was performed at 3000 *g* for 40–60 min, as detailed in the instructions.

Myocardial infarction and ES-CM transplantation

Animal protocols were approved by University of Vermont and Central Florida animal approval committees. 8–10 week-old male and female C57BL/6 mice (Taconic Farms, Hudson, NY) mice were used and divided into different study groups: Sham control (C), MI+ cell culture medium, MI+ES-CM (1x), MI+ES-CM (15x). Under general anesthesia, MI was produced as we reported previously (16). In brief, left thoracotomy was performed under sterile conditions. The mid left anterior descending (LAD) coronary artery was ligated, and the chest was closed. Sham controls were considered when some animals experienced complete surgery but no LAD ligation was performed. Cell culture medium or ES-CM was directly injected into the infarcted left ventricle at 3-5 hrs post-MI. Two intramyocardial injections of 40 μl of ES-CM or cell culture medium injections were performed at three different peri-infarct sites using a 29 gauge floating needle modified for cell delivery. The chest was closed and the animals allowed to recover. Animals were examined for echocardiography 24 h post-MI and used for further studies.

Preparation of paraffin sections and histopathology

Hearts were removed, placed in ice cold saline, fixed in 5% buffered formalin, and embedded in paraffin. Five μm serial sections were cut and used for histology. Tissue sections were deparaffinized by incubation in xylene for 5 min at room temperature, followed by transfer into fresh xylene for an additional 5 min. Sections were rehydrated using sequential incubation in 100%, 95%, and 70% ethanol for 5 min, each at room temperature, followed by washing in distilled water and phosphate-buffered saline (PBS) for 5–10 min. Heart sections were stained with standard H&E and Masson's trichrome stains.

Determination of apoptotic nuclei by TUNEL staining

Heart sections were deparaffinized as described above and permeabilized with proteinase K (25 μg/ml in 100 m*M* Tris HCl). TUNEL assay (TMR red, Roche Applied Bio Sciences) was used to determine apoptotic cell death. Negative controls were used in each case by omitting reaction mixture provided in the kit to develop staining. Sections were mounted with Antifade Vectashield mounting medium containing 4′,6-diamidino-2-phenylindole (DAPI, Vector Laboratories, Burlingame, CA) to stain nuclei. Olympus and confocal microscopes were used to identify TUNEL stained nuclei.

Quantitative analysis of apoptotic nuclei was performed on 1–2 heart sections from 4–6 different hearts as reported by us and other investigators (15, 21, 29, 33). The percentage of apoptotic nuclei per section was calculated by counting the total number of TUNEL-staining nuclei divided by the total number of DAPI-positive nuclei in 5–7 randomly selected fields at ×20 magnification.

Caspase-3 activity

Caspase-3 activity was performed using a colorimetric activity assay kit from BioVision (Mountain View, CA), as we reported previously (30, 31). In brief, LV heart tissue was removed, washed with PBS, and homogenized in the cell lysis buffer provided in the kit. Cell lysate was centrifuged and supernatants were collected for protein concentration and caspase-3 activity. The protein concentrations were determined in the supernatant using a standard colorimetric Bio-Rad assay (Hercules, CA). Caspase-3 activity was measured as per instructions detailed in the kit. Colorimetric reaction was developed and measured at 405 nm in a microtiter plate reader.

Dihydroethidium staining

Dihydroethidium (DHE) is a lipophilic dye used to measure superoxide levels in the samples, as reported (6). In brief, heart sections were deparaffinized as stated before and were incubated with DHE (1 μm/ml, Invitrogen) dye for 15–25 min in a dark chamber at room temperature. After incubation, sections were washed with PBS and counterstained with DAPI containing mounting medium. Sections were examined under Olympus and confocal fluorescence microscopes (Center Valley, PA).

c-kit, FLK-1, and CD31 immunostaining

Tissue sections were deparaffinized in xylene and rehydrated by sequential incubation in 100%, 95%, and 70% ethanol for 4 min each at room temperature, followed by washing in distilled water and phosphate-buffered saline (PBS) for 6 min. Nonspecific sites were blocked by incubation in 10% normal goat serum (NGS) for 30 min. Sections were incubated with anti-c-kit, anti-FLK-1, or with anti-CD31 mouse monoclonal antibodies (Santa Cruz Biotechnologies, Santa Cruz, CA), diluted 1:25 with 10% NGS for an hour, and followed by three washes in PBS. Next, sections were incubated with secondary antibody Alexa Fluor 568 or 488-conjugated goat anti-mouse IgG (Invitrogen) diluted 1:50 with PBS for 1 h. The sections were mounted with Vectashield antifade medium containing nuclear stain DAPI (Vector Laboratories). Quantitative analysis of c-kit^{+ve}, FLK-1^{+ve}, and CD31 was performed on heart sections from 3–5 different hearts using our Olympus and confocal fluorescence microscopes.

Coronary artery formation

Hematoxylin and eosin (H&E) and Masson's Trichrome stained heart sections were used to determine the presence of

coronary artery vessels. The cross-sectional area of the lumen of the vessel was determined by multiplying the length of the perpendicular axes measured using the grid (1–100μ, Hunt Optics, Pittsburgh, PA) loaded in the microscope eye piece and observed at 20×. The vessels with less than 50 μm^2 were classified as small, 51–300 μm^2 medium, and more than 300 μm^2 as large coronary artery vessel.

Echocardiographic analysis

Echocardiography was performed with 2%–4% isoflurane anesthesia administered via nose cone. The anesthetized animal was placed supine on a heated (37°C) imaging platform that is a component of the Visual Sonics (Toronto, CA) Vevo 770 high-resolution ultrasound imaging system. Imaging was performed with a 60 MHz probe, and two-dimensional echocardiographic images were obtained. M-mode measurements were performed for determination of anteroseptal and posterior wall thickness as well as internal dimensions during systole and diastole. From the chamber dimensions, fractional shortening ([diastolic-systolic]/diastolic) was derived.

Total antioxidant capacity assay

Antioxidants play a pivotal role in scavenging free radicals (19). There are mainly three different types of antioxidant species: enzymes (catalase, peroxidase, etc.), small molecules (vitamin E, ascorbate, uric acid, GSH, etc.), and proteins (transferrin) (14). The Bio-Vision Technologies (Exton, PA) kit used in the present study measures both small molecules antioxidants and proteins. In brief, the detection total antioxidant capacity (TAC) in CMs from ES cells or cell culture medium (control) was performed using ELISA kits in accordance with the manufacturer's instructions.

VEGF, IGF-1, and HGF ELISA assays

The detection of hepatocyte growth factor (HGF), insulin growth factor (IGF-1), and vascular endothelial growth factor (VEGF) in CMs from ES cells or cell culture medium (control) were performed using ELISA kits in accordance with the manufacturer's instructions. Kits were obtained from R&D (VEGF and IGF-1; Minneapolis, MN), and B-Bridge International (HGF; Mountain View, CA).

Data analysis

All values were expressed as means ± SE. Statistical significance was assigned when $p < 0.05$ using t-test.

Results

MIs were generated in mice hearts and ES-CMs were transplanted post-MI. To determine whether ES-CM transplantation demonstrated an anti-apoptotic effect, we performed TUNEL staining and caspase-3 activity. TUNEL staining data confirmed apoptosis in the infarcted mouse heart was significantly reduced ($p < 0.05$, Fig. 1) in the MI+ES-CMs compared with the MI+ cell culture medium-transplanted hearts. Next, we examined caspase-3 activity since it is considered a hallmark of apoptosis that plays a major role in stress-induced cardiac myocyte apoptosis. Our data confirm that caspase-3 activity was significantly reduced ($p < 0.05$, Fig. 2) in MI+ES-CMs compared with MI+cell culture medium. The reduced apoptosis confirmed with TUNEL staining in MI+ES-CM groups correlates with a decrease in caspase-3 activity post-MI. DHE staining was used as a qualitative approach to detect the generation of superoxide radicals, oxidative stress marker as reported previously (14). Our data show DHE staining was abundant in the infarcted heart sections compared with ES-CM treated groups, suggesting an increase in oxidative stress that is inhibited with ES-CM (Fig. 3).

To determine the effect of transplanted ES-CM on cardiac endogenous vascular progenitor FLK-1 cells and their contribution in enhanced neovascularization, we performed c-kit staining combined with a FLK-1 marker to identify c-kit and FLK-1 positive vascular progenitor cells. Figure 4 shows a significant increase in the combined expression of c-kit and

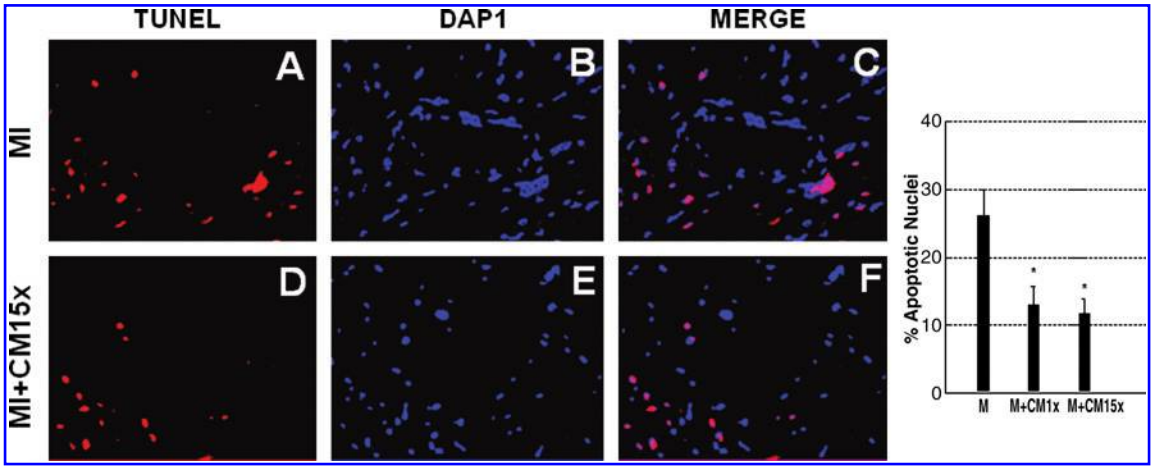

FIG. 1. Effects of transplanted ES-CM following MI on inhibited vascular cell apoptosis confirmed with TUNEL staining. Representative photomicrograph shows *red* bright immunoflurescence, apoptotic nuceli (**A** and **D**) and total nuclei stained with DAPI in *blue* (**B** and **E**). Merge images are shown in panel **C** and **F**, 40×. *Right histogram* shows quantitative number of total apoptotic nuclei in the heart are significantly reduced in MI + ES-CMs group compared with MI + cell culture medium at D1 post-MI. *$p < 0.05$ vs. MI. Data are from the set of 4–6 different animals. (For interpretation of the references to color in this figure legend, the reader is referred to the web version of this article at www.liebertonline.com/ars).

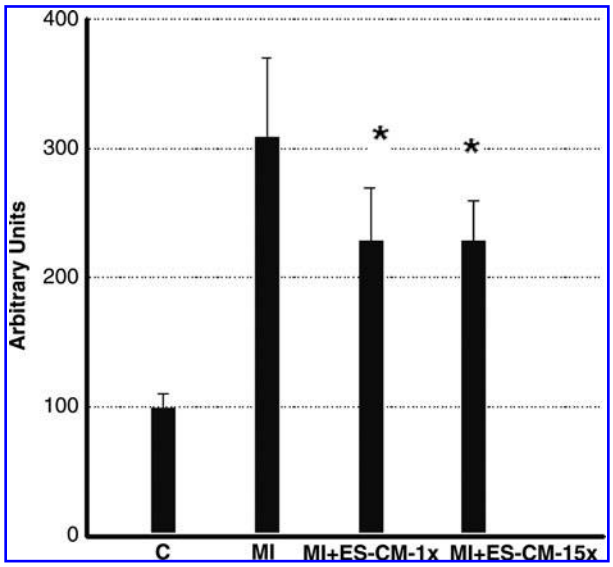

FIG. 2. Effects of transplanted ES-CM following MI on caspase-3 activity shows quantitative decrease in both 1× and 15×, MI + ES-CM groups compared with MI + cell culture medium at D1 post-MI. *$p < 0.05$ vs. MI. Data are from the set of 6 different animals.

FLK-1 stained cells in the infarcted heart following ES-CM transplantation. Our quantitative data suggest MI+ES-CM has significantly increased ($p < 0.05$, 53%) c-kit^{+ve} and FLK-1^{+ve} cells compared with MI+ cell culture medium (Fig. 4). Moreover, FLK-1 cells were also increased and were present in the small mature arteries, suggesting their contribution in repair or new artery formation in the ES-CM treated groups (data not shown). Next, we examined whether c-kit^{+ve} cells are present in mature coronary artery sites. We performed c-kit cell staining combined with CD31, a mature endothelial cell marker. Our data suggest evidences of c-kit positive cells and co-stained with mature EC marker CD31 were present in MI+ES-CM group, but no such evidences were observed in the control groups. These data suggest that transplanted ES-CM activate c-kit cells that then differentiate into mature ECs (Fig. 5). Next, immunohistochemistry staining for mature EC marker CD31 identified a 67% increase in positive cells in MI+ES-CM compared with MI+ cell culture medium (Fig. 6).

Next, we determined the effect of transplanted ES-CM on coronary artery formation. Our data shows that coronary artery formation was significantly ($p < 0.05$) increased following ES-CM transplantation (Fig. 7). Importantly, the increase was observed in small coronary arteries (<50 μm^2) in MI+ES-CM compared with MI+ cell culture groups, but no statistically significant difference was observed in the large arteries in all the groups examined (data not shown).

Echocardiography was used to examine the effects of ES-CM transplantation on cardiac function in mice at D1 post-MI. MI+ES-CM-15x group demonstrated significantly reduced LV end diastolic dimension (LVEDd) compared to MI+ cell culture medium group. MI hearts also demonstrated a significant increase in LV fractional shortening post-MI in ES-CM group compared with cell culture following transplantation (Fig. 8). Overall, the echocardiographic data suggest an improvement in cardiac function consistent with the myocardial repair and neovascularization.

Moreover, we determined the presence of c-kit activation proteins (HGF and IGF-1), anti-apoptosis factors (IGF-1 and TAC), and neovascularization protein (VEGF) using specific ELISA methods. ES-CM shows significant increase ($p < 0.05$) in levels of HGF, IGF-1, TAC, and VEGF in ES-CM compared with cell culture medium (Fig. 9). These data suggest that the presence of HGF, IGF-1, TAC, and VEGF in ES-CM compared with control medium may contribute in the inhibition of cardiovascular apoptosis and enhanced neovascularization.

Discussion

Apoptotic or necrotic cardiac myocytes and vascular cell death contribute in the development and progression of

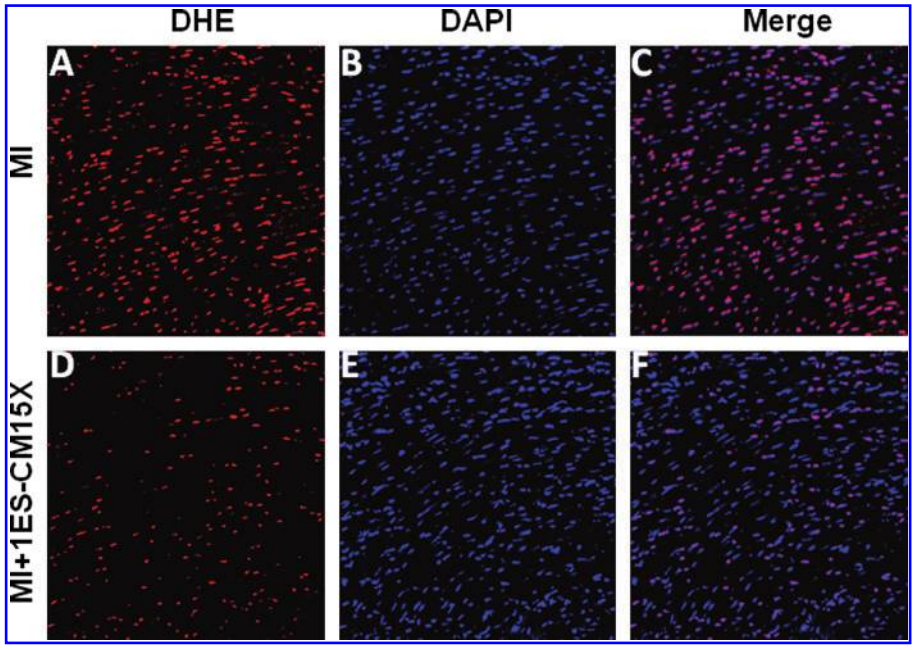

FIG. 3. Effects of transplanted ES-CM on the generation of superoxide free radicals were determined by dihydroethidium dye. Heart sections shows positive for DHE staining (**A** and **D**), total nuclei stained with DAPI in *blue* (**B** and **E**). Merged images of all three labeled sections are shown in **C** and **F** (40×). Data are from the set of 3–5 different animals. (For interpretation of the references to color in this figure legend, the reader is referred to the web version of this article at www.liebertonline.com/ars).

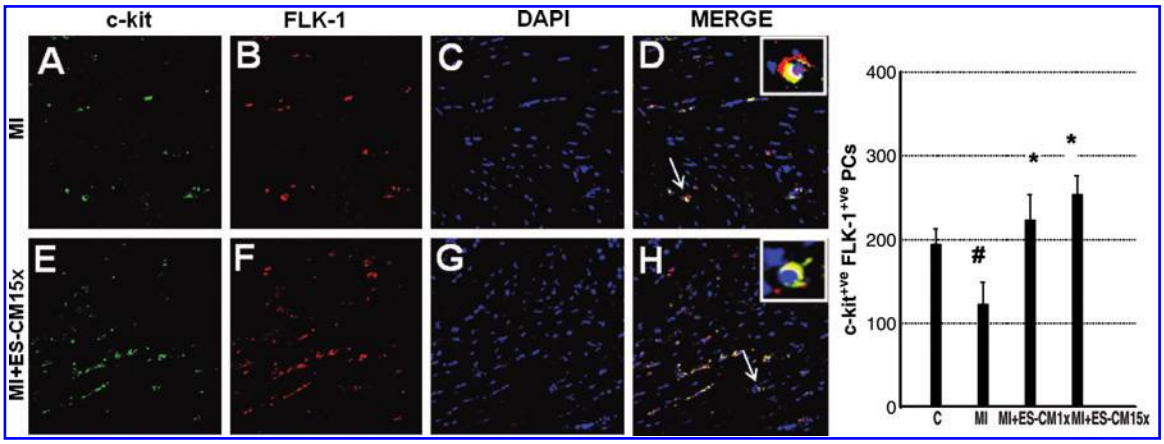

FIG. 4. Effects of transplanted ES-CM following MI on c-kit and FLK-1 stainings post-MI at D1. Representative photomicrograph shows *green* staining, c-kit^{+ve} (**A** and **E**), *red* fluorescence, FLK-1 cells (**B** and **F**), and total nuclei stained with DAPI in *blue* (**C** and **G**). Merged images of triple-labeled sections are shown in **D** and **H** (40×). *Right histogram* shows quantitative number of c-kit^{+ve} and FLK-1 positive cells significantly reduced following MI compared with sham controls. MI + ES-CM groups shows significant increase in c-kit^{+ve} and FLK-1^{+ve} cells compared with MI + cell culture medium at D1 post-MI. #$p < 0.05$, vs C *$p < 0.05$ vs. MI. Data are from the set of 3–5 different animals. (For interpretation of the references to color in this figure legend, the reader is referred to the web version of this article at www.liebertonline.com/ars).

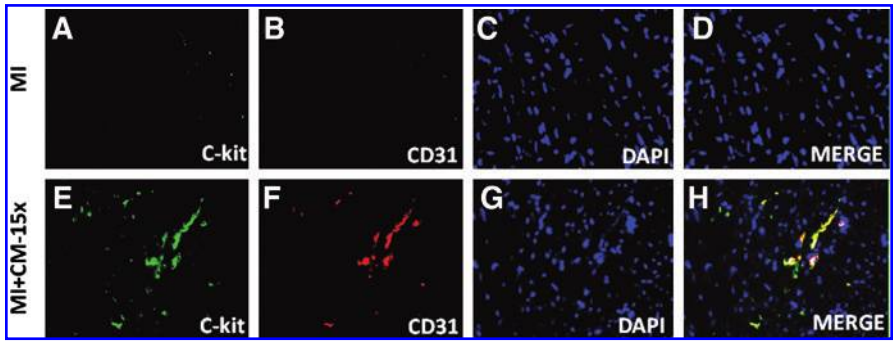

FIG. 5. Heart sections were stained for c-kit and co-labeled with endothelial cell marker CD31 antibody. Representative photomicrographs show c-kit^{+ve} staining *green* (**A** and **E**); CD31, *red* (**B** and **F**); total nuclei stained with DAPI in *blue* (**C** and **G**). Merged images of all three labeled sections are shown in **D** and **H** (40×). Data are from the set of 3–5 different animals. (For interpretation of the references to color in this figure legend, the reader is referred to the web version of this article at www.liebertonline.com/ars).

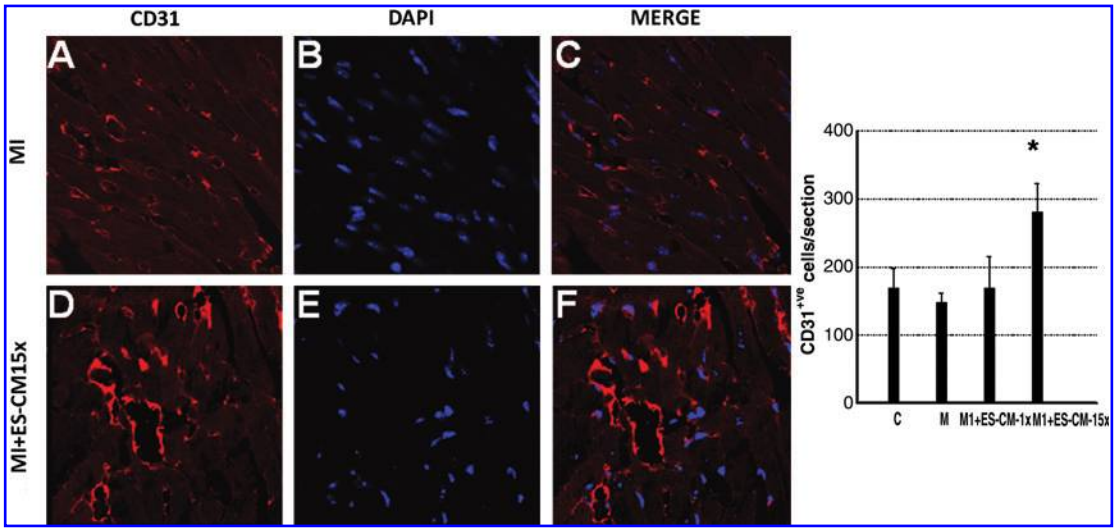

FIG. 6. Effects of transplanted ES-CM following MI on endothelial cell marker, CD31 post-MI at D1. Representative photomicrographs show *red* fluorescence, CD31 endothelial cells (**A** and **D**); total nuclei stained with DAPI in *blue* (**D** and **E**). Merged images of labeled sections are shown in **C** and **F** (40×). *Right histogram* shows quantitative number of CD31 positive cells significantly increased in MI + ES-CM-15x compared with controls. *$p < 0.05$ vs. MI. Data is from the set of 3–5 different animals. (For interpretation of the references to color in this figure legend, the reader is referred to the web version of this article at www.liebertonline.com/ars).

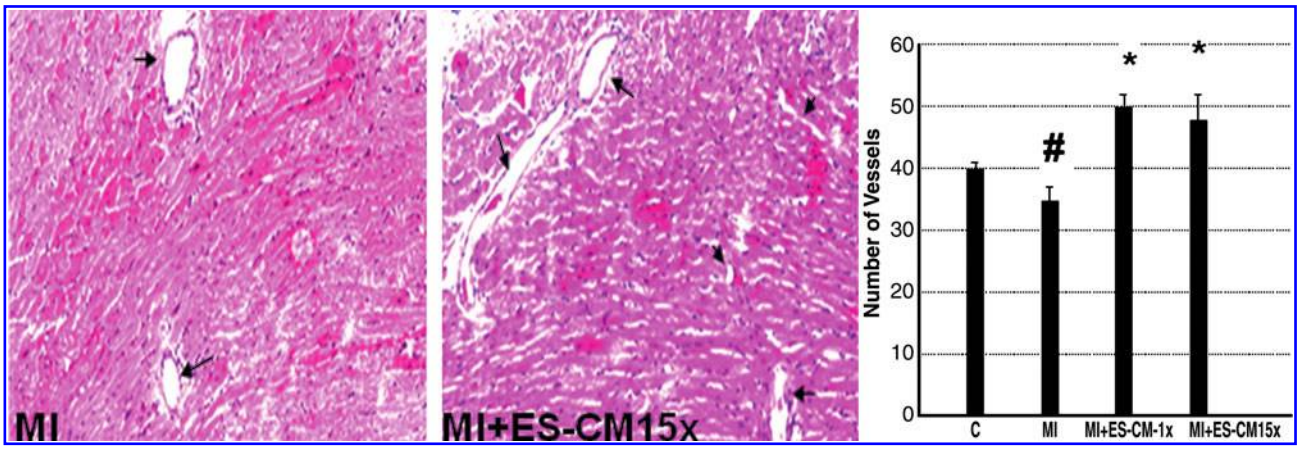

FIG. 7. Effects of transplanted ES-CM following MI on coronary artery formation post-MI. Representative photomicrographs show less number of coronary arteries are present in MI group (**A**, *arrow*) and increased number of coronary vessels were observed in ES-CM group (**B**). *Right histogram* shows quantitative number of vessels in MI and MI + ES-CM groups. #$p < 0.05$ vs C, *$p < 0.05$ vs. MI. Data are from the set of 5 different animals. (For interpretation of the references to color in this figure legend, the reader is referred to the web version of this article at www.liebertonline.com/ars).

cardiovascular disorders (1, 4, 17, 19). Oxidative stress-induced apoptosis leading to MI and heart dysfunction is well documented (1, 4, 17, 19). Moreover, inhibition of apoptosis has been reported in MI and ischemic cardiomyopathy mouse and rat models by angiotensin II inhibitors, caspase inhibitors, expression of the antiapoptotic protein Bcl-2, and antioxidants such as probucol (1, 4, 17, 19). We reported recently that transplanted ES cells in the infarcted mouse heart inhibit myocyte apoptosis and fibrosis (29). However, whether the inhibited apoptosis in the infarcted heart is mediated through autocrine or paracrine mechanisms of transplanted ES cells remains unclear. We produced ES-CM and confirmed the presence of anti-apoptotic factors released in the medium (30, 31). Released factors inhibit H_2O_2-induced apoptosis in the H9c2 cardiomyoblast cell culture model (30, 31). In the present study, our data suggest cardiac myocyte and vascular cells apoptosis, confirmed by TUNEL staining and caspase-3 activity, was significantly reduced in the ES-CM transplanted hearts. Moreover, we also observed increased amount of superoxide production in the infarcted hearts, and this increase was inhibited with ES-CM transplantation, suggesting a role of oxidative stress in increased apoptosis. Our data are consistent with the recent findings that factors released from MSCs inhibit cardiac myocyte apoptosis in the infarcted heart (7, 8). These studies suggest that reduction in post-MI apoptosis of cardiac myocytes and vascular cells in the native

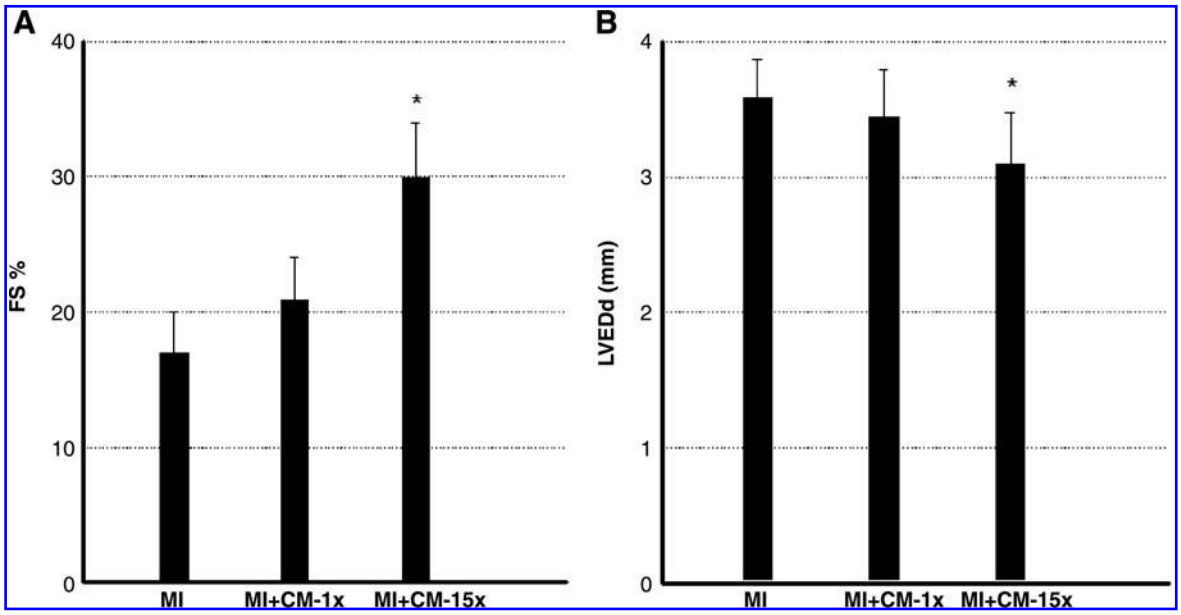

FIG. 8. Effects of ES-CM intramyocardial injection on cardiac function at D1 post-MI. *Left panel*, average echocardiographic left ventricular fractional shortening (FS); *right panel*, end diastolic diameter (LVEDd) for different treatment groups. ES cells-CM (15×) treatment was significantly different from MI ± cell culture Media group: *$p < 0.05$ vs MI.

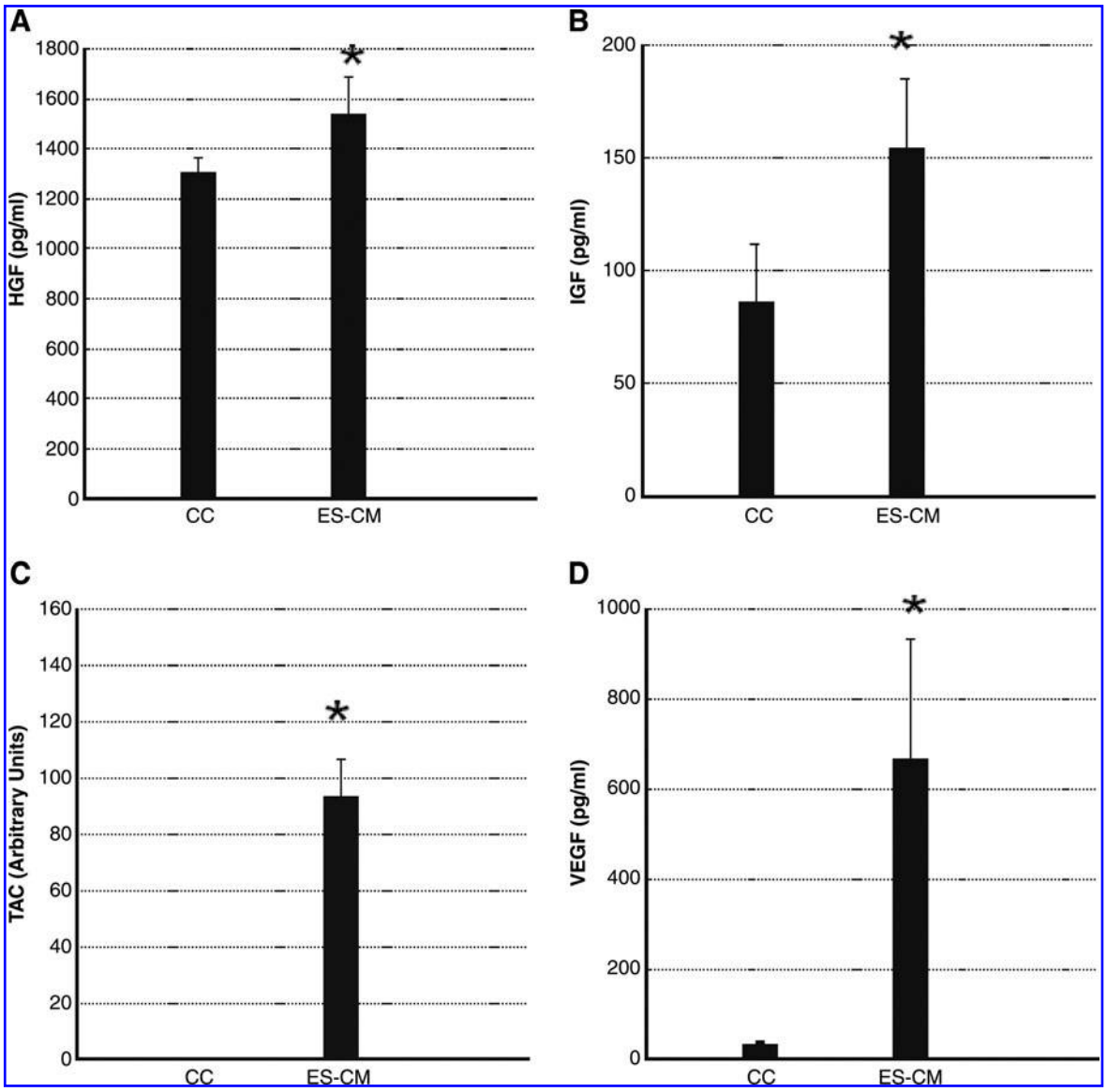

FIG. 9. Mouse hepatocyte growth factor (HGF), insulin growth factor (IGF-1), total antioxidants (TAC), and vascular endothelial growth factor (VEGF) ELISA kits were used to measure total amount of proteins present in the cell culture (CC) medium as a control, and ES-CM. Significantly increased amount of HGF (**A**), IGF-1 (**B**), TAC (**C**), and VEGF (**D**) are present in ES-CM compared with controls. Data are from 4–6 experiments. ES cells-CM shows significantly different from cell culture medium group: $^{*}p < 0.05$ vs CC.

myocardium is mediated through autocrine or paracrine action following cells transplantation (7, 8, 30, 31).

Neovascularization has been achieved with endothelial progenitor cells (EPCs) present in the peripheral blood or derived from adult and ES cell sources (20, 22, 35). Transplantation of EPCs in mouse and rat models of MI demonstrate an increase in capillary density and improved cardiac function (9, 13, 34). Similarly, G-CSF and stem cell factor (SCF) enhanced neovascularization and cardiac regeneration in mice (24). Unfortunately, clinical trials of G-CSF were unable to improve cardiac remodeling or infarct size compared with controls (25, 37). The specific stimulation of stem cells with G-CSF and contribution of EPCs in neovascularization is not clearly understood. Moreover, the effect of transplanted ES-CM on endogenous cardiac neovascularization is a new concept that remains unclear. In this context, we determined the effect of transplanted ES-CM on the stimulation of vascular progenitor cells and their role in enhanced cardiac neovascularization. In the present study, we demonstrate that ES-CM stimulates resident c-kit^{+ve} cardiac progenitor cells (CPCs) and circulating FLK-1 cells from the storage site to the injury and their differentiation into ECs. Our data are in agreement with the recent report that CPCs have the potential to differentiate into ECs and promote neovascularization following transplantation in the infarcted heart (33). Moreover, the formation and maturation of the cardiac vasculature is a multifactorial and complex process involving different cell types (35). Recently reported, FLK1-positive EPCs derived from stem cells play a major role in neovascularization in the injured myocardium and hindlimb ischemia (36). Consistent

with an important role of FLK-1 cells, we also determined whether endogenous vascular progenitors, FLK-1 cells, differentiate into mature ECs and enhance neovascularization. Our presented data suggest that ES-CM stimulate vascular progenitor FLK-1 cells and differentiate into mature ECs with enhanced neovascularization (Fig. 7).

Next, we determined the presence of anti-apoptotic and pro-angiogenic factors in ES-CM. Our ELISA data suggests that ES-CM contains increased amount of anti-apoptotic (TAC and IGF-1), and pro-angiogenic factors (IGF-1, HGF, and VEGF). So, we suggest that these released factors have provided beneficial effects in the enhanced neovascularization and inhibited apoptosis as observed in the present study. Moreover, this has shown cardiac progenitor cells primed with IGF-1 and HGF can differentiate into endothelial and VSM cells and promote neovascularization following transplantation in the infarcted heart (32). Moreover, FLK1-positive EPCs derived from stem cells have been reported to play a role in neovascularization in the injured myocardium and hindlimb ischemia (12, 26). Similarly, a recent article published in PNAS (while our paper is under review with this journal) suggests that combined growth factors of IGF-1 and VEGF following transplantation in hind limb ischemia model enhances angiogenesis and myogenesis (5). Thus, our data are consistent with recent studies suggesting that VEGF and IGF-1 enhance neovascularization.

In conclusion, this is the first study suggesting that ES-CM transplanted post-MI inhibits cardiac and vascular cell apoptosis, as well as enhance neovascularization mediated through the stimulation of endogenous cardiac and vascular progenitor cells. However, further studies are required to answer critical questions, including defining the molecular signaling pathways responsible for the neovascularization.

Acknowledgments

We acknowledge support provided by National Heart, Lung, and Blood Institute Grants 1R21-HL-085795-01A1, 1R01-HL-090646-01, and 1R01HL094467-01 (to DK Singla). The authors are thankful to Milene Brownlow for her technical help to perform part of myocardial infarction model surgeries.

Author Disclosure Statement

No competing financial interests exist.

References

1. Anversa P, Cheng W, Liu Y, Leri A, Redaelli G, and Kajstura J. Apoptosis and myocardial infarction. *Basic Res Cardiol* 93 Suppl 3: 8–12, 1998.
2. Anversa P, Kajstura J, and Olivetti G. Myocyte death in heart failure. *Curr Opin Cardiol* 11: 245–251, 1996.
3. Anversa P, Leri A, Kajstura J, and Nadal–Ginard B. Myocyte growth and cardiac repair. *J Mol Cell Cardiol* 34: 91–105, 2002.
4. Anversa P, Olivetti G, Leri A, Liu Y, and Kajstura J. Myocyte cell death and ventricular remodeling. *Curr Opin Nephrol Hypertens* 6: 169–176, 1997.
5. Borselli C, Storrie H, Benesch–Lee F, Shvartsman D, Cezar C, Lichtman JW, Vandenburgh HH, and Mooney DJ. Functional muscle regeneration with combined delivery of angiogenesis and myogenesis factors 1. *Proc Natl Acad Sci USA* 107: 3287–3292, 2010.
6. Elmarakby AA, Loomis ED, Pollock JS, and Pollock DM. NADPH oxidase inhibition attenuates oxidative stress but not hypertension produced by chronic ET-1 1. *Hypertension* 45: 283–287, 2005.
7. Gnecchi M, He H, Liang OD, Melo LG, Morello F, Mu H, Noiseux N, Zhang L, Pratt RE, Ingwall JS, and Dzau VJ. Paracrine action accounts for marked protection of ischemic heart by Akt-modified mesenchymal stem cells. *Nat Med* 11: 367–368, 2005.
8. Gnecchi M, He H, Noiseux N, Liang OD, Zhang L, Morello F, Mu H, Melo LG, Pratt RE, Ingwall JS, and Dzau VJ. Evidence supporting paracrine hypothesis for Akt-modified mesenchymal stem cell-mediated cardiac protection and functional improvement. *FASEB J* 20: 661–669, 2006.
9. Griese DP, Ehsan A, Melo LG, Kong D, Zhang L, Mann MJ, Pratt RE, Mulligan RC, and Dzau VJ. Isolation and transplantation of autologous circulating endothelial cells into denuded vessels and prosthetic grafts: Implications for cell-based vascular therapy 2. *Circulation* 108: 2710–2715, 2003.
10. Haider HK and Ashraf M. Bone marrow cell transplantation in clinical perspective. *J Mol Cell Cardiol* 38: 225–235, 2005.
11. Haider HK and Ashraf M. Bone marrow stem cell transplantation for cardiac repair. *Am J Physiol Heart Circ Physiol* 288: H2557–H2567, 2005.
12. Jujo K, Ii M, and Losordo DW. Endothelial progenitor cells in neovascularization of infarcted myocardium. *J Mol Cell Cardiol* 45: 530–544, 2008.
13. Kong D, Melo LG, Gnecchi M, Zhang L, Mostoslavsky G, Liew CC, Pratt RE, and Dzau VJ. Cytokine-induced mobilization of circulating endothelial progenitor cells enhances repair of injured arteries 2. *Circulation* 110: 2039–2046, 2004.
14. Koracevic D, Koracevic G, Djordjevic V, Andrejevic S, and Cosic V. Method for the measurement of antioxidant activity in human fluids 1. *J Clin Pathol* 54: 356–361, 2001.
15. Kudo M, Wang Y, Wani MA, Xu M, Ayub A, and Ashraf M. Implantation of bone marrow stem cells reduces the infarction and fibrosis in ischemic mouse heart. *J Mol Cell Cardiol* 35: 1113–1119, 2003.
16. Kumar D, Hacker TA, Buck J, Whitesell LF, Kaji EH, Douglas PS, and Kamp TJ. Distinct mouse coronary anatomy and myocardial infarction consequent to ligation. *Coron Artery Dis* 16: 41–44, 2005.
17. Kumar D and Jugdutt BI. Apoptosis and oxidants in the heart. *J Lab Clin Med* 142: 288–297, 2003.
18. Kumar D, Kamp TJ, and LeWinter MM. Embryonic stem cells: Differentiation into cardiomyocytes and potential for heart repair and regeneration. *Coron Artery Dis* 16: 111–116, 2005.
19. Kumar D, Lou H, and Singal PK. Oxidative stress and apoptosis in heart dysfunction. *Herz* 27: 662–668, 2002.
20. Levenberg S, Zoldan J, Basevitch Y, and Langer R. Endothelial potential of human embryonic stem cells. *Blood* 110: 806–814, 2007.
21. Li Q, Li B, Wang X, Leri A, Jana KP, Liu Y, Kajstura J, Baserga R, and Anversa P. Overexpression of insulin-like growth factor-1 in mice protects from myocyte death after infarction, attenuating ventricular dilation, wall stress, and cardiac hypertrophy. *J Clin Invest* 100: 1991–1999, 1997.
22. Loomans CJ, Wan H, de CR, van HR, de Boer HC, Leenen PJ, Drexhage HA, Rabelink TJ, van Zonneveld AJ, and Staal FJ. Angiogenic murine endothelial progenitor cells are derived from a myeloid bone marrow fraction and can be

identified by endothelial NO synthase expression. *Arterioscler Thromb Vasc Biol* 26: 1760–1767, 2006.
23. Min JY, Yang Y, Converso KL, Liu L, Huang Q, Morgan JP, and Xiao YF. Transplantation of embryonic stem cells improves cardiac function in postinfarcted rats. *J Appl Physiol* 92: 288–296, 2002.
24. Orlic D, Kajstura J, Chimenti S, Limana F, Jakoniuk I, Quaini F, Nadal-Ginard B, Bodine DM, Leri A, and Anversa P. Mobilized bone marrow cells repair the infarcted heart, improving function and survival. *Proc Natl Acad Sci USA* 98: 10344–10349, 2001.
25. Ripa RS, Jorgensen E, Wang Y, Thune JJ, Nilsson JC, Sondergaard L, Johnsen HE, Kober L, Grande P, and Kastrup J. Stem cell mobilization induced by subcutaneous granulocyte-colony stimulating factor to improve cardiac regeneration after acute ST-elevation myocardial infarction: Result of the double-blind, randomized, placebo-controlled stem cells in myocardial infarction (STEMMI) trial. *Circulation* 113: 1983–1992, 2006.
26. Sieveking DP and Ng MK. Cell therapies for therapeutic angiogenesis: Back to the bench. *Vasc Med* 14: 153–166, 2009.
27. Singla DK. Embryonic stem cells in cardiac repair and regeneration. *Antioxid Redox Signal* 11: 1857–1863, 2009.
28. Singla DK, Hacker TA, Ma L, Douglas PS, Sullivan R, Lyons GE, and Kamp TJ. Transplantation of embryonic stem cells into the infarcted mouse heart: Formation of multiple cell types. *J Mol Cell Cardiol* 40: 195–200, 2006.
29. Singla DK, Lyons GE, and Kamp TJ. Transplanted embryonic stem cells following mouse myocardial infarction inhibit apoptosis and cardiac remodeling. *Am J Physiol Heart Circ Physiol* 293: H1308–H1314, 2007.
30. Singla DK and McDonald DE. Factors released from embryonic stem cells inhibit apoptosis of H9c2 cells. *Am J Physiol Heart Circ Physiol* 293: H1590–H1595, 2007.
31. Singla DK, Singla RD, and McDonald DE. Factors released from embryonic stem cells inhibit apoptosis in H9c2 cells through P1-3kinase/Akt but not ERK pathway. *Am J Physiol Heart Circ Physiol* 295: H907–913, 2008.
32. Tillmanns J, Rota M, Hosoda T, Misao Y, Esposito G, Gonzalez A, Vitale S, Parolin C, Yasuzawa–Amano S, Muraski J, De AA, Lecapitaine N, Siggins RW, Loredo M, Bearzi C, Bolli R, Urbanek K, Leri A, Kajstura J, and Anversa P. Formation of large coronary arteries by cardiac progenitor cells. *Proc Natl Acad Sci USA* 105: 1668–1673, 2008.
33. Wang Y, Ahmad N, Wani MA, and Ashraf M. Hepatocyte growth factor prevents ventricular remodeling and dysfunction in mice via Akt pathway and angiogenesis. *J Mol Cell Cardiol* 37: 1041–1052, 2004.
34. Werner N, Priller J, Laufs U, Endres M, Bohm M, Dirnagl U, and Nickenig G. Bone marrow-derived progenitor cells modulate vascular reendothelialization and neointimal formation: Effect of 3-hydroxy-3-methylglutaryl coenzyme a reductase inhibition 3. *Arterioscler Thromb Vasc Biol* 22: 1567–1572, 2002.
35. Yamahara K and Itoh H. Potential use of endothelial progenitor cells for regeneration of the vasculature. *Ther Adv Cardiovasc Dis* 3: 17–27, 2009.
36. Yamashita J, Itoh H, Hirashima M, Ogawa M, Nishikawa S, Yurugi T, Naito M, Nakao K, and Nishikawa S. Flk1-positive cells derived from embryonic stem cells serve as vascular progenitors. *Nature* 408: 92–96, 2000.
37. Zohlnhofer D, Ott I, Mehilli J, Schomig K, Michalk F, Ibrahim T, Meisetschlager G, von WJ, Bollwein H, Seyfarth M, Dirschinger J, Schmitt C, Schwaiger M, Kastrati A, and Schomig A. Stem cell mobilization by granulocyte colony-stimulating factor in patients with acute myocardial infarction: A randomized controlled trial. *JAMA* 295: 1003–1010, 2006.

Address correspondence to:
Dinender K. Singla, Ph.D., F.A.H.A.
Associate Professor of Medicine
Burnett School of Biomedical Sciences
College of Medicine
University of Central Florida
Orlando, FL 32817

E-mail: dsingla@mail.ucf.edu

Date of first submission to ARS Central, January 20, 2010, date of final revised submission, February 23, 2010, date of acceptance, March 22, 2010.

Abbreviations Used

CC = cell culture
CPC = cardiac progenitor cells
DMEM = Dulbecco's minimum essential medium
EC = endothelial cells
ELISA = enzyme-linked Immunosorbent assay
EPCs = endothelial progenitor cells
ES-CM = embryonic stem cells conditioned medium
FLK-1 = fetal liver kinase
G-CSF = granulocyte-colony stimulating factor
H&E = hematoxylin and eosin
HGF = hepatocyte growth factor
IGF = insulin growth factor
LIF = leukemia inhibitory factor
LVEDd = left ventricular end diastolic dimension
MI = myocardial infarction
MSCs = mesenchymal stem cells
SCF = stem cell factor
TAC = total antioxidant capacity
VEGF = vascular endothelial growth factor

This article has been cited by:

1. Khawaja Husnain Haider, Muhammad AshrafPreconditioning Approach in Stem Cell Therapy for the Treatment of Infarcted Heart **111**, 323-356. [CrossRef]
2. Sarah Neel, Dinender K. Singla. 2011. Induced Pluripotent Stem (iPS) Cells Inhibit Apoptosis and Fibrosis in Streptozotocin-Induced Diabetic Rats. *Molecular Pharmaceutics* 111104095257000. [CrossRef]
3. Binbin Yan, Latifa S. Abdelli, Dinender K. Singla. 2011. Transplanted Induced Pluripotent Stem Cells Improve Cardiac Function and Induce Neovascularization in the Infarcted Hearts of db/db Mice. *Molecular Pharmaceutics* 110908085056044. [CrossRef]
4. Husnain Kh. Haider, Anique Mustafa, Yuliang Feng, Muhammad Ashraf. 2011. Genetic Modification of Stem Cells for Improved Therapy of the Infarcted Myocardium. *Molecular Pharmaceutics* 110608150833084. [CrossRef]
5. Dinender K. Singla, Xilin Long, Carley Glass, Reetu D. Singla, Binbin Yan. 2011. Induced Pluripotent Stem (iPS) Cells Repair and Regenerate Infarcted Myocardium. *Molecular Pharmaceutics* 110908084853011. [CrossRef]
6. Issei S. Shimada, Jeffrey L. Spees. 2011. Stem and progenitor cells for neurological repair: Minor issues, major hurdles, and exciting opportunities for paracrine-based therapeutics. *Journal of Cellular Biochemistry* **112**:2, 374-380. [CrossRef]